

Irreversible Magnetization Deep in the Vortex-Liquid State of a 2D Superconductor at High Magnetic Fields

T. Maniv,^{1,3} V. Zhuravlev,¹ J. Wosnitza², and J. Hagel²

¹*Chemistry Department, Technion-Israel Institute of Technology, Haifa 32000, Israel*

²*Institut für Festkörperphysik, Technische Universität Dresden, D-01062 Dresden, Germany*

³*Grenoble High Magnetic Field Laboratory, Max-Planck-Institute für Festkörperforschung and CNRS, Grenoble, France*

(Dated: February 2, 2008)

The remarkable phenomenon of weak magnetization hysteresis loops, observed recently deep in the vortex-liquid state of a nearly two-dimensional (2D) superconductor at low temperatures, is shown to reflect the existence of an unusual vortex-liquid state, consisting of collectively pinned crystallites of easily sliding vortex chains.

Many potentially important superconductors, such as some of the high- T_c cuprates, as well as the ET-based organic conductors, are extremely type-II superconductors with small in-plane coherence lengths and nearly 2D electronic structure. Thereby, ET (or BEDT-TTF) stands for bisethylenedithio-tetrathiafulvalene. Drastic deviations from the predictions of the mean-field theory for these materials, due to strong fluctuations in the superconducting (SC) order parameter, are therefore expected, in particular under strong perpendicular magnetic field [1]. The great interest, from a fundamental point of view, in the latter class of materials stems from their relatively low upper critical fields, which enable to investigate the virtually unexplored phase diagram and vortex dynamics of strongly type-II superconductors at low temperatures and high magnetic fields.

Of special interest is a recent striking observation in β'' -(ET)₂SF₅CH₂CF₂SO₃ of small, but very clear magnetization hysteresis loops appearing well above the ‘major’ irreversibility field at low temperature, where significant de Haas-van Alphen (dHvA) oscillations are observable as well [2] (Fig. 1). It should be stressed that the occurrence of such high field hysteresis tail is not peculiar to this particular material. It can also be observed at low temperatures in κ -(ET)₂Cu(SCN)₂ [3].

The unusual feature of this irreversibility effect is associated with its appearance deep in the vortex-liquid phase, where one usually expects unrestricted motion of flux lines through the entire SC sample, ensuring the establishment of thermodynamic equilibrium. In the present letter we argue that the observed hysteresis effect is a general feature which reflects the unusual nature (namely the nematic liquid-crystalline structure) of the low-temperature vortex-liquid state in 2D superconductors well above the vortex-lattice melting point, which was recently predicted theoretically [4].

According to this model the vortex state above the major irreversibility field, H_{irr} , (which is found to be close to the vortex-lattice melting field, see below) is not an isotropic liquid but some mixed phase containing SC domains of easily sliding parallel vortex chains, which are stabilized by a small number of strong pinning centers.

This model resembles the sluggish vortex fluid picture, proposed by Worthington et al [5] to describe the intermediate vortex liquid phase in defect-enhanced YBCO single crystals, and applied more recently by Sasaki et al [6] to account for a similar behavior in the organic superconductor κ -(ET)₂Cu(SCN)₂. As shown below, a simple Bean-like model for the magnetic-induction profiles, associated with the injected vortex chains into the SC sample, yields very good quantitative agreement with the measured field dependence of the magnetization hysteresis.

Our model consists of independent 2D SC layers in the x - y plane under the influence of an external uniform magnetic field $\vec{H} = H\hat{z}$, $H > 0$, perpendicular to the layers (Fig. 2). The SC sample is in contact with a normal metal at two parallel planes, $x = 0$, and $x = L_x$. H is varied, at low temperatures, from above H_{c2} to the irreversibility field $H_{irr} < H_{c2}$, where magnetic quantum oscillations can be detected. The dHvA effect is

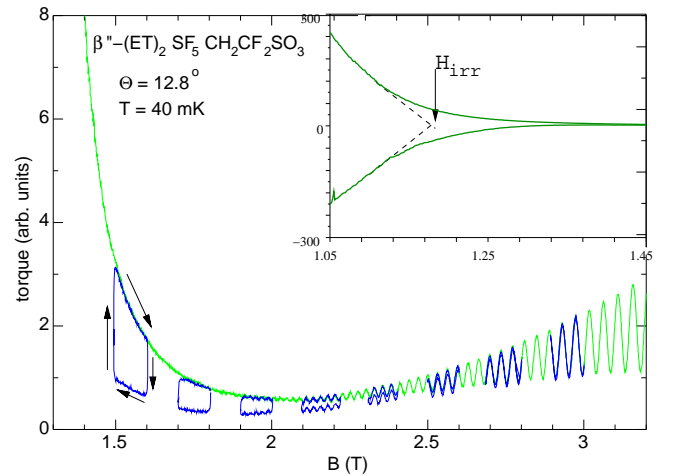


FIG. 1: Field dependence of the torque signal with several small hysteresis loops in the tail of the hysteresis loop shown in the inset. Arrows indicate the field-sweep directions. Inset: Lower field torque data showing how the major irreversibility field is determined.

measured by means of the torque method, in which the signal is detected during steady (upward and downward) sweeps of the external magnetic field. Note that, for the sake of simplicity, the small in-plane component of the external magnetic field, required for this high-resolution measurement, is neglected in our analysis.

The influence of a steady increase (or decrease) of the magnetic field on the distribution of magnetic flux lines within the SC region is determined by the pinning forces acting on quantized SC vortex lines near the normal-superconducting (N-S) boundary planes. The pinning-force resistance against flux injection leads to the establishment of a flux-density gradient perpendicular to the magnetic field direction along the normal of the N-S boundary plane (along x). Assuming the flux injection to be uniform along y , the current density $\vec{j} = j\hat{y}$ and the field gradient, $\frac{\partial \vec{B}}{\partial x}$, are connected by Ampere's law:

$$\frac{\partial \vec{B}}{\partial x} = -[\vec{\nabla} \times \vec{B}] \cdot \hat{y} = -\frac{4\pi}{c}j, \quad (1)$$

where the Lorentz-force density (per unit volume), exerted on the vortex current by the magnetic field, is

$$\vec{F}_L = \frac{1}{c}[\vec{j} \times \vec{B}] = F_L \hat{x}. \quad (2)$$

For magnetic fields below H_{irr} , the pinning force, $F_{pin} = -\frac{\partial U_{pin}}{\partial x}$, is sufficiently strong to balance the action of the driving Lorentz force, $F_L = \frac{1}{c}jB = -\frac{\partial U_L}{\partial x}$, with $U_L(x) = \frac{1}{8\pi}[B(x)]^2$, so that $\frac{\partial U_{tot}}{\partial x} = 0$, with

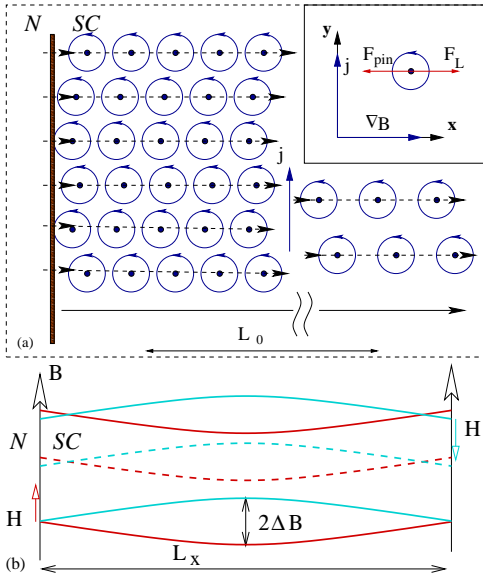


FIG. 2: (a) Sketch of a vortex crystallite, oriented with its easily sliding Bragg chains perpendicular to the N-S boundary, under injection of flux lines. Note the scaling of the magnetic length over a macroscopic distance L_0 . (b) Magnetization profiles during upward and downward field sweeps.

$U_{tot}(x) \equiv U_{pin}(x) + U_L(x)$. Consequently, the static magnetic-field gradient, $\frac{\partial \vec{B}}{\partial x}$, established across the sample, is followed by a dissipationless current parallel to the surface. This static equilibrium situation persists under the increasing local magnetic potential $U_L(x)$ near the surface, up to the ‘elastic limit’ of the pinning potential, $U_{pin}(x)$, above which bundles of vortices, accumulated near the N-S boundary, can jump over (or tunnel through) the U_{tot} -potential barriers to neighboring potential wells. Such collective vortex jumps into the SC region quickly reduce the local Lorentz force by relieving the large local field gradient, so that the movement stops after a few steps. The observed sharp magnetization jumps in this field range [2, 7] seem to be associated with this effect.

The vortex-vortex correlations in this field range are relatively strong and long ranged, so that the effective pinning force is long ranged as well. The effect is particularly significant at low pinning-center density, where these correlations can dramatically enhance collective-pinning processes, since many vortices are involved in the interaction with a single pinning center. Furthermore, due to the strong anisotropy of the vortex-vortex coupling [4], this collective-pinning mechanism is also very anisotropic. Thus, the magnetic-flux injection should encounter different resistances at different locations of the N-S boundary, depending on the local orientation of the vortex crystallite with respect to the surface. The most favorable orientation is that of crystallites having their principal lattice vector aligned perpendicular to the N-S boundary, i.e., along x , where a weak driving force can inject many vortex chains into the SC region.

As the external magnetic field approaches H_{irr} from below and the strength of the pinning potential is decreasing (because U_{pin} is proportional to the local superfluid density, which decreases with increasing B), the increasing Lorentz force can exceed the maximal value of the pinning force, i.e., the highest maximum of $U_{tot}(x)$ turns into an inflection point. Above this critical field, $U_{tot}(x)$ has no barriers and the motion of vortices in the entire SC region becomes a continuous flow. This vortex movement with velocity \vec{v}_ϕ is opposed by a dynamic friction force, $\vec{F}_\eta = -\eta\vec{v}_\phi = F_\eta \hat{x}$, which balances the action of the driving Lorentz force at the critical velocity v_ϕ^c :

$$F_L^c \equiv \frac{1}{c}j_c B = |\vec{F}_\eta| = \eta v_\phi^c. \quad (3)$$

In the corresponding steady state the motion of flux lines generates an electric field [8]

$$\vec{E} = \frac{1}{c}[\vec{B} \times \vec{v}_\phi^c] = E\hat{y}, \quad (4)$$

with $E = \frac{1}{c}Bv_\phi^c$ parallel to the current density \vec{j} . Consequently, the system develops a finite electrical resistivity to the critical-current flow, $j_c = c\eta v_\phi^c/B$, namely

$\rho(B) = E/j = B^2/c^2\eta$. Now, the Bardeen-Stephen (BS) relation [9, 10], $\eta \approx BH_{c2}/c^2\rho_n$, which is equivalent to the simple linear magnetoresistivity [8] $\rho = (B/H_{c2})\rho_n$, together with Eqs. (1) and (4), lead to:

$$\frac{\partial B}{\partial x} = - \left(\frac{4\pi H_{c2}}{c^2\rho_n} \right) v_\phi^c. \quad (5)$$

The Faraday induction law together with Eq. (4) yield the flux-line conservation law, $\frac{\partial B}{\partial t} + \frac{\partial(v_\phi B)}{\partial x} = 0$, which may be combined with Eq. (5) to obtain the nonlinear ‘diffusion’ equation for the magnetic-flux density:

$$\frac{\partial B}{\partial t} = \frac{D_\phi}{H_{c2}} \left[B \left(\frac{\partial^2 B}{\partial x^2} \right) + \left(\frac{\partial B}{\partial x} \right)^2 \right], \quad (6)$$

with the diffusion coefficient $D_\phi \equiv \frac{c^2\rho_n}{4\pi}$. In the high-field limit of interest here, when the range ΔH of a single field-sweep cycle is much smaller than the initial field of the hysteresis loop, H_0 , the nonuniform part of the magnetic induction associated with the flux flow is very small, i.e., $|b(x, t)| \equiv |B(x, t) - H(t)| \ll H(t) \simeq H_0$. Under this condition the second term on the RHS in Eq. (6) can be neglected, and the equation may be linearized to $\frac{\partial B}{\partial t} \approx \left(\frac{H_0}{H_{c2}} \right) D_\phi \frac{\partial^2 B}{\partial x^2}$. The solution of this equation, satisfying steady upward and downward field-sweep boundary conditions, $\frac{\partial B}{\partial t}(x=0, t) = \frac{\partial B}{\partial t}(x=L_x, t) = \frac{\Delta H}{\tau}$ for $0 \leq t \leq \tau$, and $-\frac{\Delta H}{\tau}$ for $\tau < t \leq 2\tau$, takes the forms: $B_+(x, t) = H_0 + \frac{\Delta H t}{\tau} + \Delta B \left[\left(\frac{2x}{L_x} - 1 \right)^2 - 1 \right]$, and $B_-(x, t) = H_0 + \Delta H \left(2 - \frac{t}{\tau} \right) - \Delta B \left[\left(\frac{2x}{L_x} - 1 \right)^2 - 1 \right]$, respectively, with τ half the period of the field-sweep cycle.

Note the spatial rigidity of the induction profiles $B_\pm(x, t)$, which is assured, in the high-field limit $|b(x, t)| \ll H$, by the nearly instantaneous propagation of any local fluctuation of the magnetic-flux density. Indeed, the propagation velocity of such a fluctuation, $v_f = \frac{\partial B}{\partial t} / \frac{\partial B}{\partial x}$, is found by Eq. (6) to be: $v_f = \frac{c^2\rho_n}{4\pi H_{c2}} \frac{\partial}{\partial x} \left(B \frac{\partial B}{\partial x} \right) / \frac{\partial B}{\partial x}$, so that the flux-line velocity v_ϕ (see Eq. (5)) satisfies: $|v_\phi| \simeq |v_f| \left(\frac{\partial B}{\partial x} \right)^2 / B \left| \frac{\partial^2 B}{\partial x^2} \right| \ll |v_f|$.

The resulting Bean-like induction profile can now be exploited to evaluate, for each small hysteresis loop, the jump, $\Delta M_{\uparrow\downarrow}$, of the magnetization occurring at a point where the field sweep is reversed (Fig. 2). The corresponding jump, $\Delta M_{\uparrow\downarrow} = \frac{\zeta}{3\pi} \Delta B$, is determined by the spatial average of the induction difference, $[B_-(x, \tau) - B_+(x, \tau)]$, where the (field-sweep rate-dependent) parameter ζ ($\zeta \leq 1$) is an effective volume fraction of the SC domains in the sample. This simple Bean-like model may be tested by estimating the parameter ρ_n , which should be identified with the in-plane resistivity at H_{c2} of the 2D conductor under study. This can be done by using the experimental values: $4\pi\Delta M_{\uparrow\downarrow} \approx 4 \times 10^{-7}$ T (see below), $L_x \approx 0.1$ cm, and $\left(\frac{\Delta H}{\tau} \right) \approx 0.005$ T/s

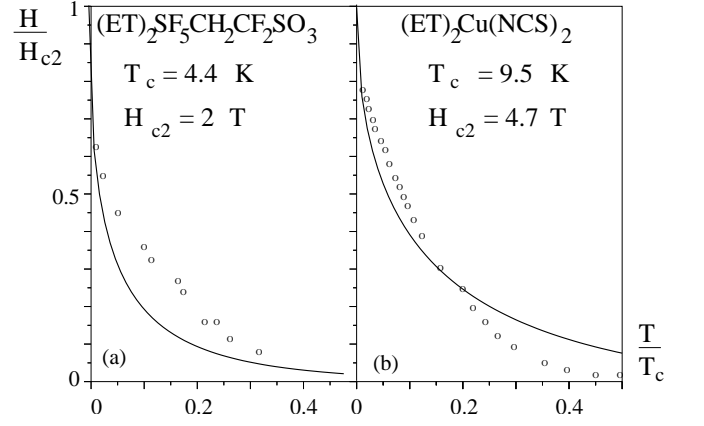


FIG. 3: Experimental major irreversibility fields (open circles), and theoretical melting fields (solid lines), as functions of temperature for two organic superconductors. Data for κ -(ET) $_2$ Cu(NCS) $_2$ from Ref. [3].

[2], in the relation $(\Delta H/\tau)\zeta = 8D_\phi(H_0/H_{c2})\Delta B/L_x^2$, which yields $\rho_n \approx \frac{\zeta L_x^2}{3c^2\Delta M_{\uparrow\downarrow}} \left(\frac{\Delta H}{\tau} \right) \approx 0.4\zeta \times 10^{-6} \Omega\text{cm}$. Assuming that ζ is of the order unity, this is a reasonable result, (i.e., of the order of a typical metallic resistivity), which cannot be easily verified experimentally, since for the very anisotropic metal under study here, measurements of the in-plane resistivity are extremely sensitive to out-of-plane scattering by a minute amount of defects.

It is interesting to estimate the characteristic energy scale corresponding to the friction of moving vortices in the liquid state above H_{irr} against the effective pinning force. This can be done by estimating the total spatial variation of the magnetic induction within the SC sample, $L_x \left| \frac{\partial B}{\partial x} \right| \approx \zeta \Delta B$, with the bar indicating spatial averaging, and comparing it to the experimental value of $\Delta M_{\uparrow\downarrow}$. Thus, the work (per unit volume) done by the driving Lorentz force against the friction force, $E_{fric} = \frac{1}{c} j_c B L_x = \frac{1}{4\pi} B \left| \frac{\partial B}{\partial x} \right| L_x \approx \frac{\zeta}{4\pi} B \Delta B$, may be rewritten in units of the maximal SC condensation-energy density, $E_{cond} = \frac{H_{c2}^2}{16\pi\kappa^2}$, that is for $B \approx H_{c2}$, $\tilde{\epsilon}_{fric} \equiv E_{fric}/E_{cond} \approx 4\kappa^2 \zeta \Delta B/H_{c2}$. Using the experimental value of the magnetization jump at 2 T, we find $\zeta \Delta B = 3\pi\Delta M_{\uparrow\downarrow} \approx 4 \times 10^{-7}$ T, so that $\tilde{\epsilon}_{fric} \approx 1.7 \times 10^{-3}$, where $\kappa \approx 46$ is used [11]. This estimate is smaller than the characteristic energy associated with the melting of the vortex lattice in 2D superconductors, which is about 2% of the SC condensation energy. It may indicate that most of the vortex crystallites are aligned with their principal lattice vector along the direction of the flux-line motion [12], so that the flux flow is dominated by easily sliding vortex chains, which are subject only to the residual shear resistance characterizing the vortex-liquid state above the melting transition [1]. This picture is very similar to the moving smectic state found recently in many numerical simulations of 2D vortex lattices in

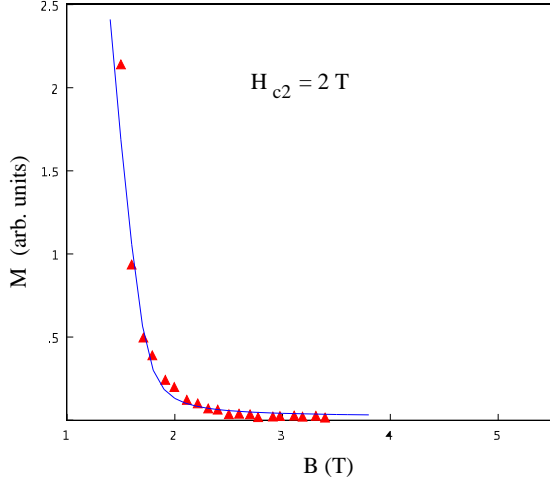


FIG. 4: Field dependences of the experimental magnetization jumps (triangles) and the fit (solid line) according to Eq. (7).

the presence of random pinning centers [13].

The value of $\tilde{\varepsilon}_{fric}$ estimated above may also reflect the correlation between the onset of irreversibility and the vortex-liquid freezing transition. This may be verified by calculating the temperature-dependent melting field, $H_m(T)$, and comparing it to the irreversible field, $H_{irr}(T)$, extracted from the experimental data. Similar to Ref. [3], $H_{irr}(T)$ is determined here by the onset of the major hysteresis in the magnetization curve (see Fig. 1). Within the Ginzburg–Landau (GL) approach, $H_m(T)$ has been derived by several authors [4, 14]. It can be obtained from $\xi^2(H_m, T) = g_m^2$, where $\xi^2(H, T) \equiv \varepsilon_0/k_B T$, with $\varepsilon_0 = \alpha^2/2\beta$ being the SC condensation energy per unit vortex, and α and β are the GL parameters [1]. Here we estimate $|\Delta_0|^2 = \frac{\alpha}{\beta} = (1.76k_B T_c)^2 \ln(\frac{H_{c2}}{B})$, and $\beta = \frac{1.38}{E_F(\hbar\omega_c)^2}$. Using our estimate, $g_m^2 \approx 1/4\lambda^2$, with $\lambda \simeq 0.066$ the effective minimal shear energy relative to ε_0 [4], and neglecting the weak temperature dependence of H_{c2} at low T , we obtain the simple equation for $h_m(t) = H_m(T)/H_{c2}(0)$: $\ln(h_m) = -k_0\sqrt{t}h_m$, where $t = T/T_c(0)$ and k_0 is a single dimensionless parameter depending on the properties of the superconductor through $k_0^2 \simeq 0.15g_m^2 E_F(\hbar\omega_{c2})^2/(k_B T_c)^3$. The function $h_m(t)$ for $\beta''\text{-(ET)}_2\text{SF}_5\text{CH}_2\text{CF}_2\text{SO}_3$, with $T_c(0) = 4.4$ K and $H_{c2} = 2$ T is shown in Fig. 3(a). The experimental irreversibility line agrees rather well with the calculated melting curve. A similar procedure is applied to $\kappa\text{-(ET)}_2\text{Cu(SCN)}_2$. The parameter $H_{c2} \approx 4.7$ T was determined by fitting the additional damping amplitude of the dHvA oscillation in the mixed SC state, as calculated from our SC fluctuations theory [1], to the corresponding experimental data [3]. Again, the calculated melting curve is found close to the irreversible line obtained in Ref. [3] [Fig. 3(b)]. It is interesting to note that at $T = 0$ the resulting melting field coincides with the mean-field

H_{c2} . The sharp increase toward H_{c2} , characterizing H_m at $T \rightarrow 0$, is similar to that of H_{irr} observed experimentally in both materials.

The relation $H_{irr} \approx H_m$ motivates us to exploit our fluctuating-vortex-chain model above H_m in calculating the magnetic-field dependence of the jump $\Delta M_{\uparrow\downarrow}$ above H_{irr} , and compare it to the experimental result (Fig. 1). Combining Eq. (1) with Eq. (3), we may rewrite the critical gradient as $|\partial B/\partial x| = 4\pi|F_\eta|/B = 4\pi E_{fric}/L_x B$. Since the generators of the friction force, i.e., the pinning force and the vortex-vortex interactions, all originate in the existence of local SC order at the vortex position, the friction energy E_{fric} should be proportional to the mean-square SC order parameter, $\langle|\Delta_0(H)|^2\rangle$, and so the magnetization jump can be written as $\Delta M_{\uparrow\downarrow} = \frac{\zeta}{3\pi}\Delta B \approx \frac{L_x}{3\pi}|\frac{\partial B}{\partial x}| \propto \frac{1}{B}\langle|\Delta_0(B)|^2\rangle$. Using the limit of independently fluctuating vortex chains in the GL theory [1] to describe the vortex-liquid state above H_{irr} , i.e., writing: $\langle|\Delta_0(B)|^2\rangle = \sqrt{\frac{2k_B T}{\pi^2\beta}}\Phi(\xi)$, where $\Phi(\xi) = \sqrt{\pi}\left[\xi + \frac{\exp(-\xi^2)}{2\int_{-\infty}^{\xi} d\zeta \exp(-\zeta^2)}\right]$, we find that

$$\Delta M_{\uparrow\downarrow} \propto \frac{1}{B}\langle|\Delta_0(B)|^2\rangle \propto \Phi(\xi) \quad (7)$$

is a universal function of the dimensionless parameter $\xi(B, T)$. Employing the material parameters, $T_c = 4.4$ K, $\frac{m_c}{m_e} = 2.0$, $E_F/k_B = 133$ K at the temperature of the experiment, $T = 40$ mK, so that $\xi \approx 31(1 - B/H_{c2})/B$, and treating H_{c2} and the proportionality factor in Eq. (7) as adjustable parameters, the best fit is obtained for $H_{c2} = 2$ T (Fig. 4). The resulting curve reflects the crossover between the vortex-crystal state below H_{c2} , which is well described by mean-field theory, and the normal state far above H_{c2} , with the long tail of the field-dependent magnetization hysteresis corresponding to the enhanced influence of 2D SC fluctuations.

In conclusion, we have shown that the striking phenomenon of the weak magnetization hysteresis loops, observed deep in the vortex-liquid state of a nearly 2D superconductor can be reasonably explained as arising from shear viscous flow of easily sliding vortex chains, which are clustered around a small number of strong pinning centers.

This research was supported by a grant from the Israel Science Foundation founded by the Academy of Sciences and Humanities, and by the fund from the promotion of research at the Technion.

-
- [1] T. Maniv, V. Zhuravlev, I.D. Vagner, and P. Wyder, *Rev. Mod. Phys.* **73**, 867 (2001).
 - [2] J. Wosnitzer *et al.*, *Phys. Rev. B* **67**, 060504(R) (2003).
 - [3] T. Sasaki *et al.*, *Phys. Rev. B* **57**, 10889 (1998).
 - [4] V. Zhuravlev and T. Maniv, *Phys. Rev. B* **66**, 014529 (2002); *ibid.* **60**, 4277 (1999).

- [5] T.K. Worthington et al., Phys. Rev. B **46**, 11854 (1992)
- [6] T. Sasaki et al., Phys. Rev. B **66**, 224513-1 (2002).
- [7] M.M. Mola *et al.*, Phys. Rev. Lett. **86**, 2130 (2001).
- [8] A.A. Abrikosov, *Fundamentals of the Theory of Metals* (North-Holland Pub., Amsterdam 1988).
- [9] J. Bardeen and M.J. Stephen, Phys. Rev. A **1197** (1965).
- [10] For a review see: G. Blatter *et al.*, Rev. Mod. Phys. **66**, 1125 (1994).
- [11] S. Wanka *et al.*, Phys. Rev. B **57**, 3084 (1998). The value $\kappa \approx 46$ is recalculated using the reduced value of H_{c2} found in the present paper.
- [12] C. Reichhardt and G.T. Zimanyi, Phys. Rev. B **61**, 14354 (2000).
- [13] O.J. Olson, C. Reichardt and F. Nori, Phys. Rev. Lett. **81**, 3757 (1998).
- [14] Z. Tesanovic and L. Xing, Phys. Rev. Lett. **67**, 2729 (1991); Y. Kato and N. Nagaosa, Phys. Rev. B **48**, 7383 (1993); J. Hu and A.H. MacDonald, Phys. Rev. Lett. **71**, 432 (1993).